

A Temporal Estimate of Integrated Information for Intracranial Functional Connectivity

Xerxes D. Arsiwalla^{1,2,4}, Daniel Pacheco^{1,2,4}, Alessandro Principe³,
Rodrigo Rocamora³, and Paul Verschure^{2,4,5}

¹ Universitat Pompeu Fabra, Barcelona, Spain

² Institute for BioEngineering of Catalonia, Barcelona, Spain

³ Hospital del Mar, Barcelona, Spain

⁴ Barcelona Institute of Science and Technology, Barcelona, Spain

⁵ Institució Catalana de Recerca i Estudis Avançats (ICREA), Barcelona, Spain
{x.d.arsiwalla@gmail.com}

Abstract. A major challenge in computational and systems neuroscience concerns the quantification of information processing at various scales of the brain’s anatomy. In particular, using human intracranial recordings, the question we ask in this paper is: How can we estimate the informational complexity of the brain given the complex temporal nature of its dynamics? To address this we work with a recent formulation of network integrated information that is based on the Kullback-Leibler divergence between the multivariate distribution on the set of network states versus the corresponding factorized distribution over its parts. In this work, we extend this formulation for temporal networks and then apply it to human brain data obtained from intracranial recordings in epilepsy patients. Our findings show that compared to random re-wirings of the data, functional connectivity networks, constructed from human brain data, score consistently higher in the above measure of integrated information. This work suggests that temporal integrated information may indeed be a good starting point as a future measure of cognitive complexity.

Keywords: Computational Neuroscience; Brain Networks; Complexity Measures; Functional Connectivity

1 Introduction

The human brain is an extremely complex non-linear dynamical system that processes information from the external world, coming in through sensory channels, in order to determine the sequence of actions necessary for goal-oriented behavior, given the agent’s internal drives and emotional states. Investigating the mechanisms of information integration, flow and distribution provide a vital ingredient in advancing our understanding of brain function and cognition. This is point at which information theory meets neuroscience. The former provides rigorous theoretical tools that can effectively be employed to quantify biophysical processes that encode and assimilate knowledge from the world, which is then

used to generate goal-oriented action. In this paper, we focus on quantifying the amount of information integrated by functional connectivity networks constructed from local field potentials (LFPs) obtained using intracranial recordings from human epilepsy patients. The underlying non-linearities in neural processing are reflected in the fact that these functional connectivity (FC) networks are not static, but dynamic. For our purposes, this can be analyzed as a stack of temporal networks, signifying the multitude of functional states the brain can occupy. This also calls for new dynamical measures of information processing to investigate these temporal networks.

Such measures are part of a larger class of complexity measures that seek to quantify information generated by all causal sub-processes in such a network. One candidate measure for global information processing is integrated information, usually denoted as Φ . It was introduced as a complexity measure for neural networks, and by extension, as a possible correlate of consciousness itself [30]. It is defined as the quantity of information generated by a network as a whole, due to its causal dynamical interactions, and one that is over and above the information generated independently by the disjoint sum of its parts. As a complexity measure, Φ seeks to operationalize the intuition that complexity arises from simultaneous integration and differentiation of the network's structural and dynamical properties. The earliest proposals defining integrated information were made in the pioneering work of [30], [29] and [27]. Since then, considerable progress has been made towards development of a normative theory of consciousness as well as applications of integrated information [15], [17], [28], [1], [23], [8], [11], [4], [5], [7], [9], [6], [10]. In fact, there are now several candidate measures of integrated information such as neural complexity [30], causal density [25], Φ from integrated information theory: IIT 1.0, 2.0 & 3.0 [27], [15], [23], stochastic interaction [31], [14], empirical Φ [17] and synergistic Φ [22], plus several variations of these (see [26] for an overview).

We will work with a recent formulation of network integrated information that is based on the Kullback-Leibler divergence between the multivariate distribution on the set of network states versus the corresponding factorized distribution over its parts [12]. This formulation is particularly suited for large networks with stochastic dynamics. In this paper, we extend this formulation for temporal networks. Note that in an ideal setting, to use the measure in [12] one would need the realistic anatomical connectivity of neural populations generating LFPs as well as details of the non-linear model generating those dynamics. In the absence of both these pieces of information, we rely on temporal FC networks as proxy to the realistic non-linear processes in the brain and compute the temporal integrated information of these networks.

2 Mathematical Formulation of Integrated Information

Let us begin this discussion considering networks endowed with linear stochastic dynamics. The state of each node is given by a random variable pertaining to a given probability distribution. These variables may either be discrete-valued

or continuous. However, for many biological applications, Gaussian distributed, continuous-valued state variables are fairly reasonable abstractions (for example, aggregate neural population firing rate, EEG or fMRI signals). The state of the network \mathbf{X}_t at time t is taken as a multivariate Gaussian variable with distribution $\mathbf{P}_{\mathbf{X}_t}(\mathbf{x}_t)$. \mathbf{x}_t denotes an instantiation of \mathbf{X}_t with components x_t^i (i going from 1 to n , n being the number of nodes). When the network makes a transition from an initial state \mathbf{X}_0 to a state \mathbf{X}_1 at time $t = 1$, observing the final state generates information about the system's initial state. The information generated equals the reduction in uncertainty regarding the initial state \mathbf{X}_0 . This is given by the conditional entropy $\mathbf{H}(\mathbf{X}_0|\mathbf{X}_1)$. In order to extract that part of the information generated by the system as a whole, over and above that generated individually by its parts, one computes the relative conditional entropy given by the Kullback-Leibler divergence of the conditional distribution $\mathbf{P}_{\mathbf{X}_0|\mathbf{X}_1=\mathbf{x}'}(\mathbf{x})$ of the system with respect to the joint conditional distributions $\prod_{k=1}^r \mathbf{P}_{\mathbf{M}_0^k|\mathbf{M}_1^k=\mathbf{m}'}$ of its non-overlapping sub-systems demarcated with respect to a partition \mathcal{P}_r of the system into r distinct sub-systems. Denoting this as $\Phi_{\mathcal{P}_r}$, we have

$$\Phi_{\mathcal{P}_r}(\mathbf{X}_0 \rightarrow \mathbf{X}_1 = \mathbf{x}') = D_{KL} \left(\mathbf{P}_{\mathbf{X}_0|\mathbf{X}_1=\mathbf{x}'} \parallel \prod_{k=1}^r \mathbf{P}_{\mathbf{M}_0^k|\mathbf{M}_1^k=\mathbf{m}'} \right) \quad (1)$$

where for an r partitioned system, the state variable \mathbf{X}_0 can be decomposed as a direct sum of state variables of the sub-systems

$$\mathbf{X}_0 = \mathbf{M}_0^1 \oplus \mathbf{M}_0^2 \oplus \dots \oplus \mathbf{M}_0^r = \bigoplus_{k=1}^r \mathbf{M}_0^k \quad (2)$$

and similarly, \mathbf{X}_1 decomposes as

$$\mathbf{X}_1 = \mathbf{M}_1^1 \oplus \mathbf{M}_1^2 \oplus \dots \oplus \mathbf{M}_1^r = \bigoplus_{k=1}^r \mathbf{M}_1^k \quad (3)$$

For stochastic systems, it is useful to work with a measure that is independent of any specific instantiation of the final state \mathbf{x}' . So we average with respect to final states to obtain an expectation value from eq.(1). After some algebra, we get

$$\langle \Phi \rangle_{\mathcal{P}_r}(\mathbf{X}_0 \rightarrow \mathbf{X}_1) = -\mathbf{H}(\mathbf{X}_0|\mathbf{X}_1) + \sum_{k=1}^r \mathbf{H}(\mathbf{M}_0^k|\mathbf{M}_1^k) \quad (4)$$

This is our definition of integrated information, which we use in the rest of this paper. Note that the measure described in [15] is not applicable to networks with stochastic dynamics. They do use eq.(1) as their definition but endow their nodes with discrete states. On the other hand, [17] uses a different definition of integrated information, where conditional entropies as in eq.(4) are replaced by conditional mutual information. This definition only matches the definition of eq.(1) in special cases but not in general for any distribution. From an information theory perspective, the Kullback-Leibler divergence offers a principled

way of comparing probability distributions, hence we follow that approach in formulating our measure in eq.(4).

The state variable at each time $t = 0$ and $t = 1$ follows a multivariate Gaussian distribution

$$\mathbf{X}_0 \sim \mathcal{N}(\bar{\mathbf{x}}_0, \Sigma(\mathbf{X}_0)) \quad \mathbf{X}_1 \sim \mathcal{N}(\bar{\mathbf{x}}_1, \Sigma(\mathbf{X}_1)) \quad (5)$$

The generative model for this system is equivalent to a multi-variate autoregressive process

$$\mathbf{X}_1 = \mathcal{A} \mathbf{X}_0 + \mathbf{E}_1 \quad (6)$$

where \mathcal{A} is the weighted adjacency matrix of the network and E_1 is Gaussian noise. Next, taking the mean and covariance respectively on both sides of this equation, while holding the residual independent of the regression variables, yields

$$\bar{\mathbf{x}}_1 = \mathcal{A} \bar{\mathbf{x}}_0 \quad \Sigma(\mathbf{X}_1) = \mathcal{A} \Sigma(\mathbf{X}_0) \mathcal{A}^T + \Sigma(\mathbf{E}) \quad (7)$$

In the absence of any external inputs, stationary solutions of a stochastic linear dynamical system as in eq.(6) are fluctuations about the origin. Therefore, we can shift coordinates to set the means $\bar{\mathbf{x}}_0$ and consequently $\bar{\mathbf{x}}_1$ to the zero. The second equality in eq.(7) is the discrete-time Lyapunov equation and its solution will give us the covariance matrix of the state variables.

The conditional entropy of a multivariate Gaussian variable is computed to be

$$\mathbf{H}(\mathbf{X}_0|\mathbf{X}_1) = \frac{1}{2}n \log(2\pi e) - \frac{1}{2} \log [\det \Sigma(\mathbf{X}_0|\mathbf{X}_1)] \quad (8)$$

which is fully specified by the conditional covariance matrix. Inserting this in eq.(4) yields

$$\langle \Phi \rangle_{\mathcal{P}_r}(\mathbf{X}_0 \rightarrow \mathbf{X}_1) = \frac{1}{2} \log \left[\frac{\prod_{k=1}^r \det \Sigma(\mathbf{M}_0^k|\mathbf{M}_1^k)}{\det \Sigma(\mathbf{X}_0|\mathbf{X}_1)} \right] \quad (9)$$

To compute the conditional covariance matrix we use the following identity (the proof for the Gaussian case can be found in [16])

$$\Sigma(\mathbf{X}|\mathbf{Y}) = \Sigma(\mathbf{X}) - \Sigma(\mathbf{X}, \mathbf{Y})\Sigma(\mathbf{Y})^{-1}\Sigma(\mathbf{X}, \mathbf{Y})^T \quad (10)$$

The appropriate covariance we will need to insert in this expression is

$$\Sigma(\mathbf{X}_0, \mathbf{X}_1) \equiv \langle (\mathbf{X}_0 - \bar{\mathbf{x}}_0)(\mathbf{X}_1 - \bar{\mathbf{x}}_1)^T \rangle = \Sigma(\mathbf{X}_0) \mathcal{A}^T \quad (11)$$

which gives for the conditional covariance

$$\Sigma(\mathbf{X}_0|\mathbf{X}_1) = \Sigma(\mathbf{X}_0) - \Sigma(\mathbf{X}_0) \mathcal{A}^T \Sigma(\mathbf{X}_1)^{-1} \mathcal{A} \Sigma(\mathbf{X}_0)^T \quad (12)$$

And similarly for the sub-systems

$$\Sigma(\mathbf{M}_0^k|\mathbf{M}_1^k) = \Sigma(\mathbf{M}_0^k) - \Sigma(\mathbf{M}_0^k) \mathcal{A}^T|_k \Sigma(\mathbf{M}_1^k)^{-1} \mathcal{A}|_k \Sigma(\mathbf{M}_0^k)^T \quad (13)$$

where k indexes the partition such that \mathbf{M}_0^k denotes the k^{th} sub-system at $t = 0$ and $\mathcal{A}|_k$ denotes the restriction of the adjacency matrix to the k^{th} sub-network.

Further, for linear multi-variate systems, a unique fixed point always exists. We try to find stable stationary solutions of the dynamical system. In that regime, the multi-variate probability distribution of states approaches stationarity and the covariance matrix converges, such that

$$\Sigma(\mathbf{X}_1) = \Sigma(\mathbf{X}_0) \quad (14)$$

$t = 0$ and $t = 1$ refer to time-points taken after the system converges to the fixed point. Then the discrete-time Lyapunov equations can be solved iteratively for the stable covariance matrix $\Sigma(\mathbf{X}_t)$. For networks with symmetric adjacency matrix and independent Gaussian noise, the solution takes a particularly simple form

$$\Sigma(\mathbf{X}_t) = (\mathbf{1} - \mathcal{A}^2)^{-1} \Sigma(\mathbf{E}) \quad (15)$$

and for the parts, we have

$$\Sigma(\mathbf{M}_0^k) = \Sigma(\mathbf{X}_0)|_k \quad (16)$$

given by the restriction of the full covariance matrix on the k^{th} sub-network. Note that eq.(16) is not the same as eq.(15) on the restricted adjacency matrix as that would mean that the sub-network has been explicitly severed from the rest of the system. Indeed, eq.(16) is precisely the covariance of the sub-network while it is still part of the network and $\langle \Phi \rangle$ yields the integrated and differentiated information of the whole network that is greater than the sum of these connected parts. Inserting eqs.(12), (13), (15) and (16) into eq.(9) yields $\langle \Phi \rangle$ as a function of network weights for symmetric and correlated networks. For the case of asymmetric weights, the entries of the covariance matrix cannot be explicitly expressed as a matrix equation. However, they may still be solved by Jordan decomposition of both sides of the Lyapunov equation.

For partitioning the network, we will use the Maximum Information Partition (MaxIP). Following [21] and [1], the MaxIP is defined as the partition of the system into its irreducible parts. This is the finest partition and is unique as there is only one way to combinatorially reduce a system into all of its sub-units. $\langle \Phi \rangle$ computed using this partition was shown to accounts for the maximum amount of information that the network can integrate compared to any other partitioning of the system and is therefore a natural choice for quantifying whole versus parts [12].

3 Experimental Protocol

Intracranial EEG data for a single subject performing a navigation task was collected as part of a pre-surgical procedure in an epileptic patient. The participant provided written informed consent to participate in the study. The protocol of

the experiment was approved by the local Ethical Committee "Clinical Research Ethical Committee (CEIC) Parc de Salut Mar" (Barcelona, Spain). Recordings were performed using a standard clinical EEG system (XLTEK, subsidiary of Natus Medical) with 500 Hz sampling rate. A unilateral implantation was performed, using 10 intra-cerebral electrodes (Dixi Medical, Besancon, France; diameter: 0.8 mm; 5 to 15 contact points, 2 mm long, 1.5 mm apart) that were stereotactically inserted using robotic guidance (ROSA, Medtech Surgical, Inc).

The subject navigated a squared virtual environment in which discrete visual stimuli were presented at specific locations in a 5x5 grid formed by red boxes located on the ground. Navigation was performed with a joystick. Boxes remained visible during the whole navigation period. When subjects were close to one of the boxes, the item pertaining to that specific location was presented through a small inset in the top-right of the user interface. Participants were instructed to visit all boxes. The subject completed six blocks of three minutes each. Navigation data (i.e., positions and orientations) of the subject during the active condition was recorded at 1000 Hz. We band-pass filtered the signal for the selected electrodes from 1 to 200 Hz using EEGLAB [20] before building the FCs. Functional correlation matrices were constructed by binning the activity of all electrodes in sliding windows of 500 ms. We calculated the Spearman's correlation of the activity of all pairs of electrodes over time. Electrode localization included frontal, parietal and temporal lobes, including brain structures such as the hippocampus and the amygdala (these locations were checked using the BrainX³ system [13], [3], [24], [18], [19], [2]). After filtering the data for removal of artifacts, we were left with a stack of 1797 FC networks of size 60x60.

4 Results

As described above, the data extraction process gives us a stack of 1797 temporal networks. We apply the mathematical machinery of integrated information to this stack. The measure being defined at each time-point yields a profile of $\langle\Phi\rangle$ values reflecting variations in informational complexity across time. As mentioned earlier, we use the structure of these temporal FC networks as proxy to the underlying complex neural connectivity and dynamics. Eq.(9) is computed at each time-point using the corresponding FC network as the connectivity matrix \mathcal{A} . We use all positive correlations for this analysis. Furthermore, network weights are normalized by an overall scaling factor of 19.2 for all networks in order to ensure that all eigenvalues of all networks are bounded by 1 for reasons of stability. This yields the temporal $\langle\Phi\rangle$ profile for the FC networks, shown in red in fig. 1. As a possible null model, we randomize the data by shuffling the edges of each FC network while preserving the total network degree at each point of time. Computing $\langle\Phi\rangle$ for these randomized networks yields the green profile in fig. 1. Fig. 2 shows the corresponding histograms of these $\langle\Phi\rangle$ profiles.

Given these profiles, we can now perform test statistics on $\langle\Phi\rangle$ itself in order to compare the temporal FC with their randomized counterparts. More, generally this method may also be used for making statistical statements for $\langle\Phi\rangle$ under

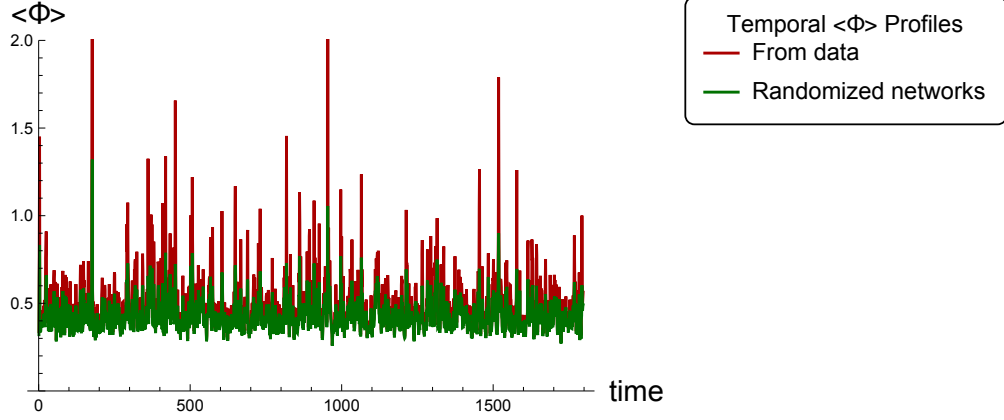


Fig. 1. Temporal $\langle \Phi \rangle$ for data (red profile) versus randomized networks (green profile) Here $\langle \Phi \rangle$ is computed as bits of information, while time runs in steps of 100ms.

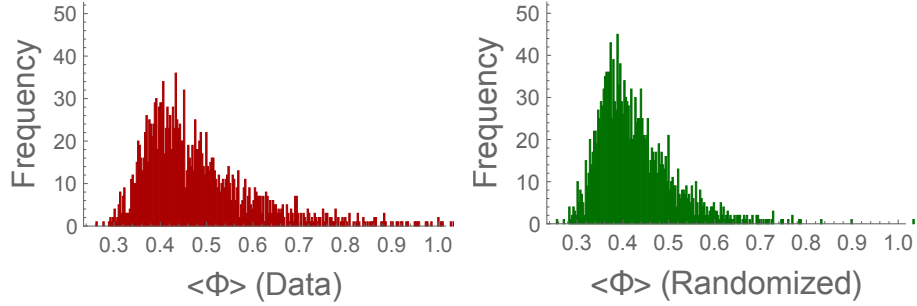


Fig. 2. Histograms of $\langle \Phi \rangle$ for data (left) and randomized networks (right)

different experimental conditions. We compute the mean, median and variance of the $\langle \Phi \rangle$ profiles for both the data and the randomized case. Since the $\langle \Phi \rangle$ profiles do not follow a normal distribution, we use then use the Mann-Whitney-Wilcoxon test to compare the medians between the two $\langle \Phi \rangle$ profiles and we find a significant difference in favor of the brain FCs. For comparing the variances we employ the Brown-Forsythe test (for non-parametric and non-symmetric distributions) and again find significant difference in favor of the data. Our results are shown in table 1 below. What these results show is that integrated information is a useful measure for quantifying the plethora of patterns observed in temporal FC networks corresponding to various brain states. Compared to random rewirings, the original FC networks scored consistently higher values of $\langle \Phi \rangle$ with a greater mean and median (statistically significant). Additionally, the data networks show a much greater variance (statistically significant) in $\langle \Phi \rangle$ than their random counterparts. This suggests that realistic temporal FC networks of the

Table 1. Test statistics on $\langle\Phi\rangle$ profiles showing the median, mean and variance in values of $\langle\Phi\rangle$ for brain data versus the randomized network. The last column shows p-values for each test.

	$\langle\Phi\rangle$ (FC)	$\langle\Phi\rangle$ (Randomized)	p-value
Median	0.45	0.41	$< 10^{-40}$
Mean	0.51	0.43	N.A.
Variance	0.28	0.01	$< 10^{-20}$

brain explore a greater region of state space than random configurations. For future work, it might be interesting to look closer at the occasional strong peaks in $\langle\Phi\rangle$ that we observe in the FC networks, which may be driven either by task complexity or by spontaneous neural activity.

5 Discussion

Information-based methods offer a useful way to quantify complexity of brain functions. Integrated information is interesting as a global measure of a system’s collective behavior. In this work, we extend the computational framework of network integrated information for temporal networks and applied it to local field potential (LFP) data obtained from human intracranial recordings. This generates a time-series profile of Φ reflecting the dynamical nature of the brain’s informational complexity. As a null model we generate another profile of Φ obtained from randomizing the FC networks at each instance of time (while preserving total degree for each network). This enables a statistical comparison of complexity under two conditions. More specifically, for brain functional networks we find that compared to random re-wirings, the original FC networks scored consistently higher values of $\langle\Phi\rangle$ with a greater mean and median (statistically significant). Additionally, the data networks show a much greater variance (statistically significant) in $\langle\Phi\rangle$ than their random counterparts, thus suggesting that realistic temporal FC networks of the brain explore a greater region of state space than random configurations. This work demonstrates that temporal integrated information may be a good starting point as a future measure of cognitive complexity. This can have potential impact in the clinic for identifying information-based differences between healthy subjects and patients of neurodegenerative diseases.

Acknowledgments. This work is supported by the European Research Council’s CDAC project: ”The Role of Consciousness in Adaptive Behavior: A Combined Empirical, Computational and Robot based Approach”, (ERC-2013- ADG 341196).

References

1. Arsiwalla, X.D., Verschure, P.F.M.J.: Integrated information for large complex networks. In: The 2013 International Joint Conference on Neural Networks (IJCNN). pp. 1–7 (Aug 2013)
2. Arsiwalla, X.D., Betella, A., Bueno, E.M., Omedas, P., Zucca, R., Verschure, P.F.: The dynamic connectome: A tool for large-scale 3d reconstruction of brain activity in real-time. In: ECMS. pp. 865–869 (2013)
3. Arsiwalla, X.D., Dalmazzo, D., Zucca, R., Betella, A., Brandi, S., Martinez, E., Omedas, P., Verschure, P.: Connectomics to semantomics: Addressing the brain’s big data challenge. *Procedia Computer Science* 53, 48–55 (2015)
4. Arsiwalla, X.D., Herreros, I., Moulin-Frier, C., Sanchez, M., Verschure, P.F.: Is Consciousness a Control Process?, pp. 233–238. IOS Press, Amsterdam (2016)
5. Arsiwalla, X.D., Herreros, I., Verschure, P.: On Three Categories of Conscious Machines, pp. 389–392. Springer International Publishing, Cham, Switzerland (2016)
6. Arsiwalla, X.D., Mediano, P.A., Verschure, P.F.: Spectral modes of network dynamics reveal increased informational complexity near criticality. *Procedia Computer Science* 108, 119–128 (2017)
7. Arsiwalla, X.D., Moulin-Frier, C., Herreros, I., Sanchez-Fibla, M., Verschure, P.F.: The morphospace of consciousness. arXiv preprint arXiv:1705.11190 (2017)
8. Arsiwalla, X.D., Verschure, P.: Computing Information Integration in Brain Networks, pp. 136–146. Springer International Publishing, Cham, Switzerland (2016)
9. Arsiwalla, X.D., Verschure, P.: Why the brain might operate near the edge of criticality. In: International Conference on Artificial Neural Networks. pp. 326–333. Springer (2017)
10. Arsiwalla, X.D., Verschure, P.: Measuring the complexity of consciousness. *Frontiers in Neuroscience* 12, 424 (2018)
11. Arsiwalla, X.D., Verschure, P.F.M.J.: High Integrated Information in Complex Networks Near Criticality, pp. 184–191. Springer International Publishing, Cham, Switzerland (2016)
12. Arsiwalla, X.D., Verschure, P.F.: The global dynamical complexity of the human brain network. *Applied Network Science* 1(1), 16 (2016)
13. Arsiwalla, X.D., Zucca, R., Betella, A., Martinez, E., Dalmazzo, D., Omedas, P., Deco, G., Verschure, P.: Network dynamics with brainx3: A large-scale simulation of the human brain network with real-time interaction. *Frontiers in Neuroinformatics* 9(2) (2015)
14. Ay, N.: Information geometry on complexity and stochastic interaction. *Entropy* 17(4), 2432–2458 (2015)
15. Balduzzi, D., Tononi, G.: Integrated information in discrete dynamical systems: motivation and theoretical framework. *PLoS Comput Biol* 4(6), e1000091 (2008)
16. Barrett, A.B., Barnett, L., Seth, A.K.: Multivariate granger causality and generalized variance. *Physical Review E* 81(4), 041907 (2010)
17. Barrett, A.B., Seth, A.K.: Practical measures of integrated information for time-series data. *PLoS Comput Biol* 7(1), e1001052 (2011)
18. Betella, A., Bueno, E.M., Kongsantad, W., Zucca, R., Arsiwalla, X.D., Omedas, P., Verschure, P.F.M.J.: Understanding large network datasets through embodied interaction in virtual reality. In: Proceedings of the 2014 Virtual Reality International Conference. pp. 23:1–23:7. VRIC ’14, ACM, New York, NY, USA (2014)
19. Betella, A., Cetnarski, R., Zucca, R., Arsiwalla, X.D., Martínez, E., Omedas, P., Mura, A., Verschure, P.F.M.J.: Brainx3: Embodied exploration of neural data. In:

- Proceedings of the 2014 Virtual Reality International Conference. pp. 37:1–37:4. VRIC '14, ACM, New York, NY, USA (2014)
20. Delorme, A., Makeig, S.: Eeglab: an open source toolbox for analysis of single-trial eeg dynamics including independent component analysis. *Journal of neuroscience methods* 134(1), 9–21 (2004)
 21. Edlund, J.A., Chaumont, N., Hintze, A., Koch, C., Tononi, G., Adami, C.: Integrated information increases with fitness in the evolution of animats. *PLoS Comput Biol* 7(10), e1002236 (2011)
 22. Griffith, V., Koch, C.: Quantifying Synergistic Mutual Information, pp. 159–190. Springer Berlin Heidelberg, Berlin, Heidelberg (2014), http://dx.doi.org/10.1007/978-3-642-53734-9_6
 23. Oizumi, M., Albantakis, L., Tononi, G.: From the phenomenology to the mechanisms of consciousness: integrated information theory 3.0. *PLoS Comput Biol* 10(5), e1003588 (2014)
 24. Omedas, P., Betella, A., Zucca, R., Arsiwalla, X.D., et al: Xim-engine: A software framework to support the development of interactive applications that uses conscious and unconscious reactions in immersive mixed reality. In: Proceedings of the 2014 Virtual Reality International Conference. pp. 26:1–26:4. VRIC '14, ACM, New York, NY, USA (2014)
 25. Seth, A.K.: Causal connectivity of evolved neural networks during behavior. *Network: Computation in Neural Systems* 16(1), 35–54 (2005)
 26. Tegmark, M.: Improved measures of integrated information. arXiv preprint arXiv:1601.02626 (2016)
 27. Tononi, G.: An information integration theory of consciousness. *BMC neuroscience* 5(1), 42 (2004)
 28. Tononi, G.: Integrated information theory of consciousness: an updated account. *Arch Ital Biol* 150(2-3), 56–90 (2012)
 29. Tononi, G., Sporns, O.: Measuring information integration. *BMC neuroscience* 4(1), 31 (2003)
 30. Tononi, G., Sporns, O., Edelman, G.M.: A measure for brain complexity: relating functional segregation and integration in the nervous system. *Proceedings of the National Academy of Sciences* 91(11), 5033–5037 (1994)
 31. Wennekers, T., Ay, N.: Stochastic interaction in associative nets. *Neurocomputing* 65, 387–392 (2005)